Thermochimica Acta 501 (2010) 35–45

Contents lists available at ScienceDirect

Thermochimica Acta

journal homepage: www.elsevier.com/locate/tca

Advanced kinetics for calorimetric techniques and thermal stability screening of sulfide minerals

Abduljelil Iliyas*, Kelly Hawboldt, Faisal Khan

Faculty of Engineering and Applied Science, Memorial University of Newfoundland, St. John's, N.L., Canada A1B 3X5

ARTICLE INFO

Article history:
Received 7 October 2009
Received in revised form
17 December 2009
Accepted 21 December 2009
Available online 28 January 2010

Keywords:
Sulfide minerals
Oxidation kinetics
Self-heating
DSC
Iso-conversional methods
MLA

ABSTRACT

Thermal methods of analysis such as differential scanning calorimetry (DSC) provide a powerful methodology for the study of solid reactions. This paper proposes an improved thermal analysis methodology for thermal stability investigation of complex solid-state reactions. The proposed methodology is based on differential iso-conversional approach and involves peak separation, individual peak analysis and combination of isothermal/non-isothermal DSC measurements for kinetic analysis and prediction. The proposed thermal analysis, which coupled with Mineral Libration Analyzer (MLA) technique was employed to investigate thermal behavior of sulfide mineral oxidation. The importance of various experimental variables such as particle size, heating rate and atmosphere were investigated and discussed. The information gained from such an advanced thermal analysis method is useful for scale-up processes with potential of significant savings in plant operations, as well as in mitigating adverse environmental and safety issues arising from handling and storage of sulfide minerals.

1. Introduction

Study of sulfide mineral oxidation, characterization of the reactions involved, and prediction of the fate of sulfide oxidation products in natural environments, during processing, storage, and shipping are increasingly becoming active areas of research. Locally severe environmental and safety issues associated with sulfide mineral oxidation in part motivate this growing research interest.

Previous publications have attempted to propose mechanisms, and hence obtain kinetics for the different reactions associated with sulfide mineral oxidation using sophisticated instruments. While such kinetics might be useful under prevailing experimental conditions, they may not be capable of extrapolation to pilot or industrial scale studies [1]. This is due to the significant influence of experimental variables on reaction mechanisms involving solid-state reactions. Several researchers [2–4] have reported that parameters such as particle size, gas environments and heating rates considerably influence reaction mechanisms during sulfide mineral oxidation, such that tests conducted under a given set of conditions will provide reaction sequences valid for that set of conditions, and may not necessarily be extendable to other conditions.

Alternatives to expensive spectroscopic instruments are simple calorimetric techniques, such as differential scanning calorimetry (DSC) and differential thermal analysis (DTA) for kinetic investigation. Although the latter approach has been in use for over three decades, recent advances in computation techniques have heightened interest in DSC/DTA and associated thermal analysis methods. It has been demonstrated in previous studies [1,5,6] that under well-controlled experimental conditions, apparent kinetic information of complex reactions can be obtained using DSC without necessarily discriminating between reaction sequences/mechanisms. The obtained kinetic information is useful in predicting thermal behavior of larger scale processes.

In the present work, we employed an iso-conversional kinetic approach to investigate thermal stability/behavior of sulfide mineral concentrates using DSC apparatus. An advanced iso-conversional based approach is proposed for kinetic parameter estimation. This approach involves separating overlapping endo/exothermic events, subsequent to kinetic analysis of each event, and combining measurements from isothermal and non-isothermal regimes for kinetic analysis.

2. Experimental

Two fresh samples (1–2) were obtained directly from Voisey's Bay Mine, Vale-Inco Newfoundland and Labrador, while two weathered ones (3–4) were obtained from a local hydromet processing plant. The samples were screened for thermal stability in a DSC system (Q-100 series from TA Instruments). The DSC was calibrated with the manufacturer supplied sapphire disk and indium

* Corresponding author. Tel.: +1 709 737 7652; fax: +1 709 737 6193.
E-mail address: ajiliyas@mun.ca (A. Iliyas).

0040-6031/$ – see front matter.
doi:10.1016/j.tca.2009.12.020

Table 1
Sample mineralogical compositions.

Sample	Particle size (μm)	Pre-oxidized phase (wt%)	Pentlandite (wt%)	Pyrrhotite (wt%)	Chalcopyrite (wt%)	Others (wt%)
1	<25	40.5	30.9	16.9	7.4	4.3
2	60–70	31.9	50	13.1	2.4	2.6
3	80–110	35.6	52.6	9.6	0.5	1.7
4	80–110	39.2	46.4	10.5	1.6	2.3

standard following the instrument calibration guidelines. In the dynamic mode of operation, approximately 10 mg of each sample is subjected to temperature ramp at 0.5, 1, 3, and 5 K/min heating rates under isobaric conditions with oxygen (10 ml/min) as the purge gas. To ensure that the observed DSC exotherm is mainly due to oxidation, a test is repeated at 5 K/min in nitrogen environment, and with platinum-lined cell under similar conditions.

The isothermal tests were conducted at 130, 145 and, 160 °C. In the isothermal test, the DSC sample holder is heated to the desired temperature, after which it is rapidly opened and the pre-weighed sample immediately placed on the sample holder. The system is allowed to equilibrate at desired isothermal temperature before data collection is initiated.

2.1. Numerical tools

The advanced thermokinetic software package AKTS – Thermokinetics and Thermal Safety Software [7] was used for this study. The software suite is based on differential iso-conversional techniques. Baseline subtraction is a major problem in kinetic analysis of DSC thermogram, however, the AKTS software tool is capable of performing baseline optimization simultaneously with thermokinetic parameters determination. Thus, increasing the accuracy of estimated thermokinetic parameters. Details on the numerical optimization routine of the software can be found in Ref. [7].

3. Results

3.1. SEM-MLA

Particle de-agglomeration and phase segregation were achieved using Mineral Libration Analyzer (MLA) techniques to distinguish between the different mineral phases (or grains). Backscattered electron (BSE) images of the as-received concentrates shown in Fig. 1 revealed that the particles consist of pentlandite (iron–nickel

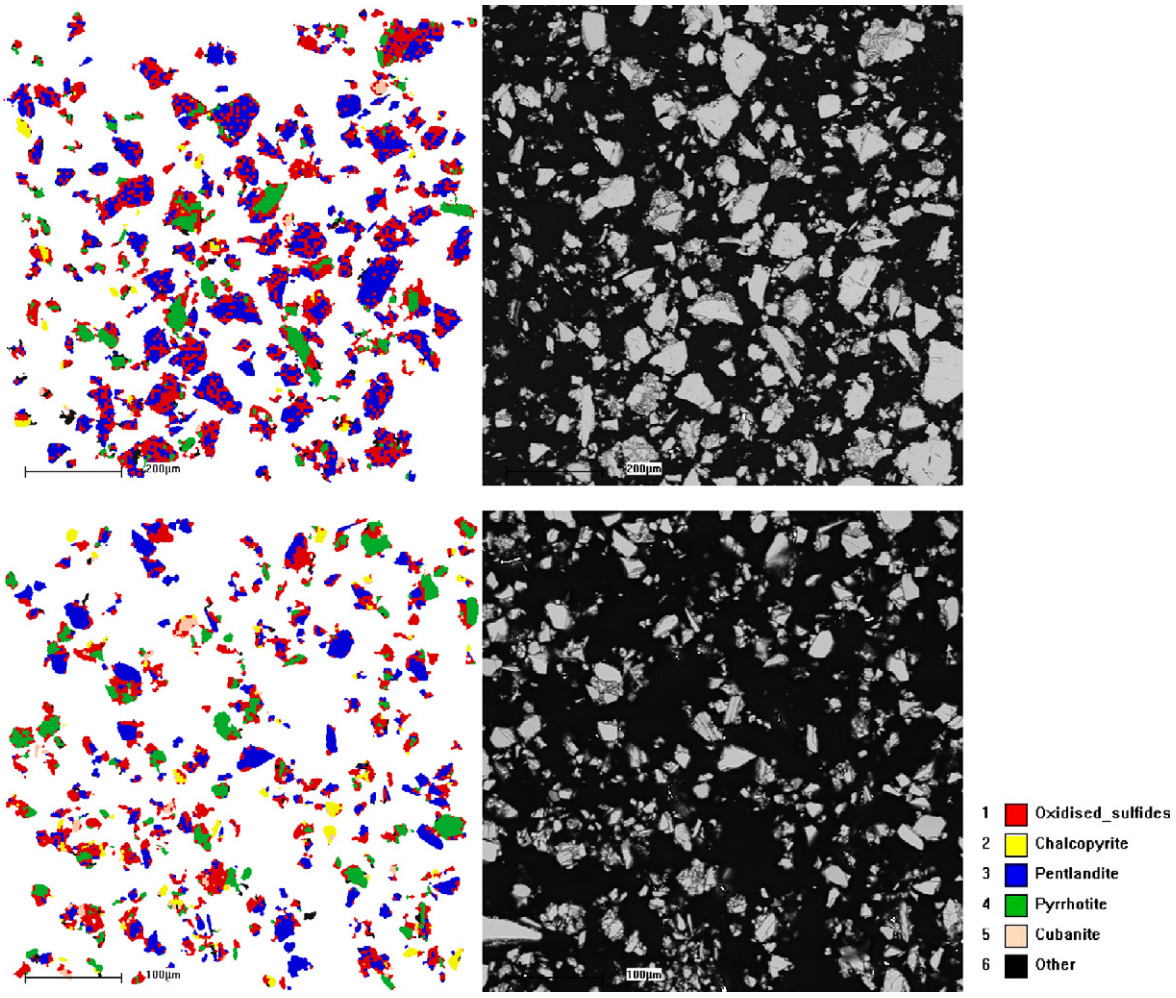

Fig. 1. Backscattered electron images of representative mineral concentrate sample showing pentlandite as main sulfide phase with smaller grains of other minerals.

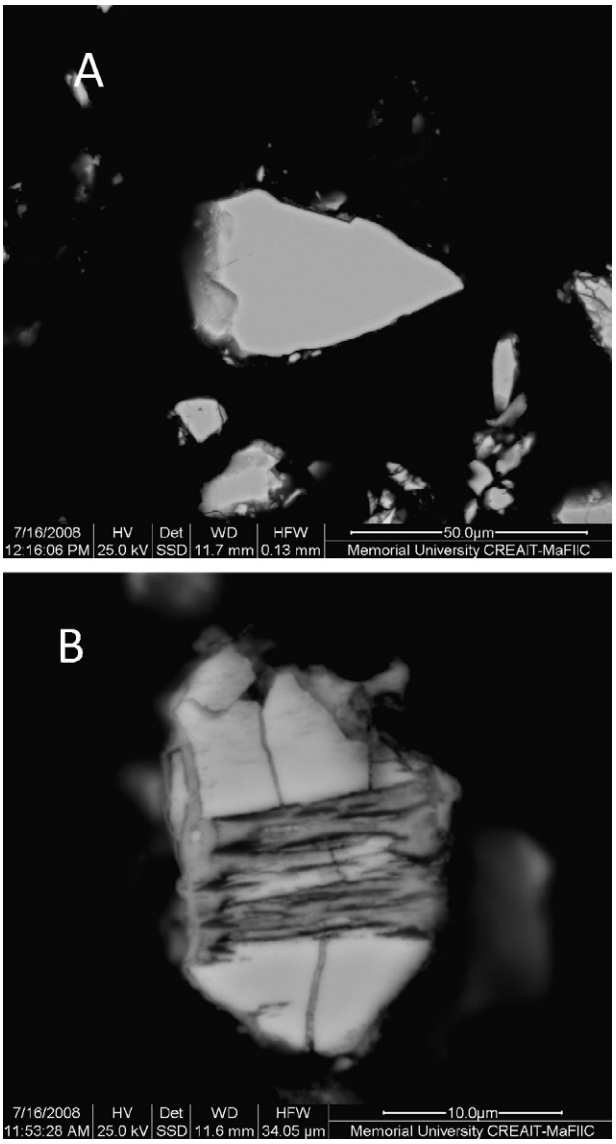

Fig. 2. Enlarged BSE image of (A) un-oxidized and (B) partially oxidized particle. Note the alterations running across the width and/or along the length of the oxidized particle.

sulfide) and smaller grains of pyrrhotite (iron sulfide), chalcopyrite and cubanite (copper–iron sulfides) – see also Table 1. The pre-oxidized sulfide implies sample oxidation before arriving at our lab. The enlarged BSE image of a typical unreacted particle revealed a smooth, metallic luster surface free of cavities as shown in Fig. 2A. The image of partially reacted particles shows that oxidation results in particle alterations with veins of an oxidized phase running either across the width and/or along the length of the particle (Fig. 2B). This is in agreement with the image collected by Thornhill and Pidgeon [8] in a study of sulfide mineral roasting. They reported that the particles are oxidizing preferentially along certain crystallographic planes. This result differs from the reported BSE images of sulfide mineral ores [9], which show preferential oxidation along the rims/margins of the particles. Note that the particle shown in Fig. 2B contain areas of apparently unreacted sulfide. This is likely because the rate of the oxidation of these areas is significantly slower than those placed along certain crystallographic planes.

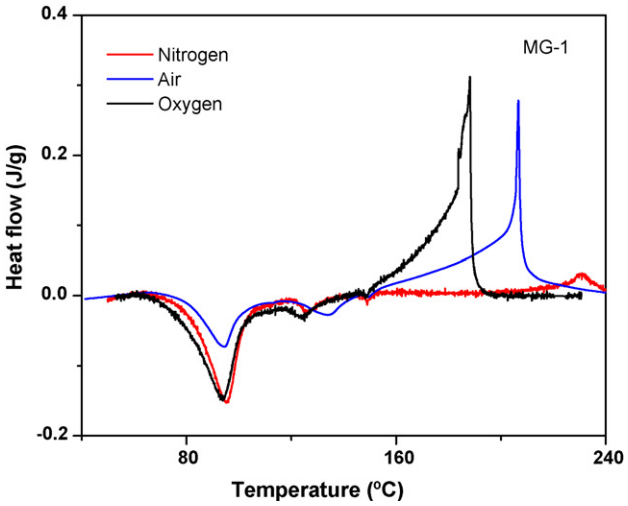

Fig. 3. Effect of gas enviroment on the non-isothermal DSC signals at 5 K/min for representative mineral concentrate (sample 2).

3.2. DSC measurements of sulfide minerals oxidation

Fig. 3 shows the DSC signals for a representative concentrate sample heated in different gas environment at 5 K/min. The first endothermic event appears to be independent of oxygen partial pressure possibly suggesting an irreversible reaction. In contrast, the magnitude and maximum of the exothermic event was clearly affected by different gas environments, i.e., shifted towards higher temperature with decreasing oxygen partial pressures clearly indicating a solid–gas reaction as suggested by the parametric sensitivity of thermal analysis reported in Ref. [10].

Fig. 4 shows the obtained DSC signals for the four samples at different heating rates in oxygen environment. Several thermal events, including multiple endotherms and exotherms are apparent with all the samples. Depending on the heating rates, the first and second endotherms appear between 46–120 and 90–160 °C respectively. These endothermic events are possibly related to desulfuration, which was reported to precede the exothermic reaction [3,11,12]. This explanation seemed reasonable considering that some sulfide minerals contain non-stoichiometric sulfur, e.g., pyrrhotite that would readily be decomposed into stoichiometric sulfide with sulfur liberation.

Exothermic events associated with sulfide mineral (MS) oxidation have been widely studied [4,9,13–16]. A common conclusion from these studies is the formation of SO_2 from a highly exothermic reaction that is readily detected as an exothermic peak in the DSC/DTA record. The reaction can be expressed in general as [1]:

$$2MS_{(s)} + 3O_{2(g)} \rightarrow 2MO_{(s)} + 2SO_{2(g)}$$

In the present study, the major exothermic events were observed between 110 and 220 °C for the concentrate samples. The exothermic peaks recorded in this study exhibit considerably earlier temperature onset (by over 150 °C) than those reported in Ref. [9]. This is not surprising considering the difference between procedural variables used in the cited references and this study, such as oxidizing conditions, sample composition, particle size distribution and heating rates. The present study was conducted in vigorous oxidizing conditions to better capture the complexity of the concentrates oxidation (as depicted in Fig. 3), as well to obtain parameters under "worse-case" scenario for subsequent safety prediction.

Comparing the oxidative behavior of the different samples, it can be seen from Fig. 4 that samples 1 and 2 featured multiple

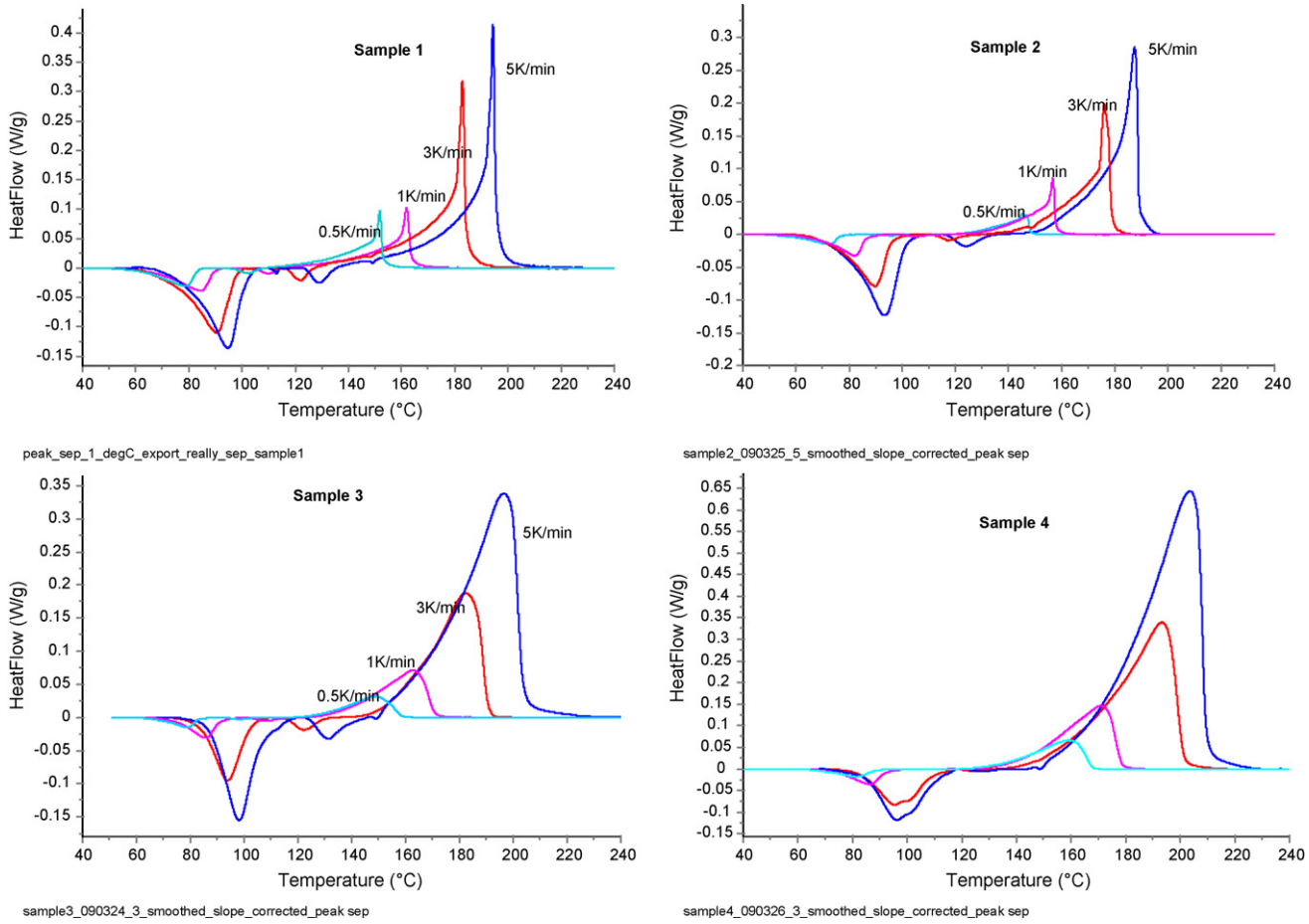

Fig. 4. Obtained DSC signals from non-isothermal measurements in oxygen environment at different heating rates.

overlapping peaks with sharp gradients, whereas broader gradients are apparent with samples 3 and 4. Dunn and Kelly [17] observed a similar multiple overlapping exothermic peaks for pentlandite oxidation in O_2 environment, which they attributed to side reactions taking place in concert with the major reaction, e.g., pentlandite break down to Fe_2O_3, $NiSO_4$, NiO, NiS and $NiFe_2O_4$ with SO_2 evolution. Similar reactions are likely to occur with samples used in this study considering that pentlandite constitutes a major reactive phase in all the samples (Table 1). However, since additional minerals are also present in our samples, other reactions cannot be ruled out.

Determining the reaction chemistry of the concentrate oxidation demands complex investigation using comparative methods, which is beyond the scope of this paper. The objective of the present study is to obtain apparent kinetic information for mineral sulfide oxidation. As demonstrated in subsequent sections of this paper, postulating schemes for individual reactions involved in oxidation is not necessary to attain this objective with differential iso-conversional kinetic approach employed herein.

3.3. Kinetic analysis

To obtain an accurate estimation of the reaction kinetics, we deemed it is necessary to separate the endothermic/exothermic peaks particularly if an overlap occurs to eliminate uncertainties in selecting the evaluation range, which may adversely affect baseline optimization. This was achieved by fitting the Gaussian and/or Fraser–Suzuki (asymmetric) types signals to the experimental data using non-linear optimization (Marquardt) routine in the advanced thermokinetic software package – AKTS. The results are displayed as peak optimal parameters with the graphical presentation of the fitted curves and the separated peaks depicted in Fig. 5.

Following peak separation, the endothermic and exothermic signals were optimized for baseline correction while simultaneously applying differential iso-conversional techniques. The mathematical description of applied differential iso-conversional approach is discussed in greater details elsewhere [18].

Fig. 6 shows iso-conversional plots for the first endothermic event of all samples while the corresponding apparent activation energy variations with reaction progress for this event is presented

Table 2
Estimated enthalpy changes and apparent activation ranges for different DSC thermal events.

Sample	Particle size (μm)	Endothermic (46–120 °C)		Endothermic (90–160 °C)		Exothermic (110–220 °C)	
		ΔH_r (J/g)	E_a (kJ/mol)	ΔH_r (J/g)	E_a (kJ/mol)	ΔH_r (J/g)	E_a (kJ/mol)
1	<25	33.8 ± 8.2	129–210	4.8 ± 2.6	114–110	73.5 ± 30.7	55–88
2	60–70	24.3 ± 1.3	92–107	1.7 ± 0.63	105–63	38.4 ± 4.1	73–105
3	80–110	21.9 ± 1.5	83–123	3.1 ± 0.7	83–67	83.9 ± 9.0	72–93
4	80–110	27.0 ± 0.5	80–113	–	–	170.8 ± 16.9	80–94

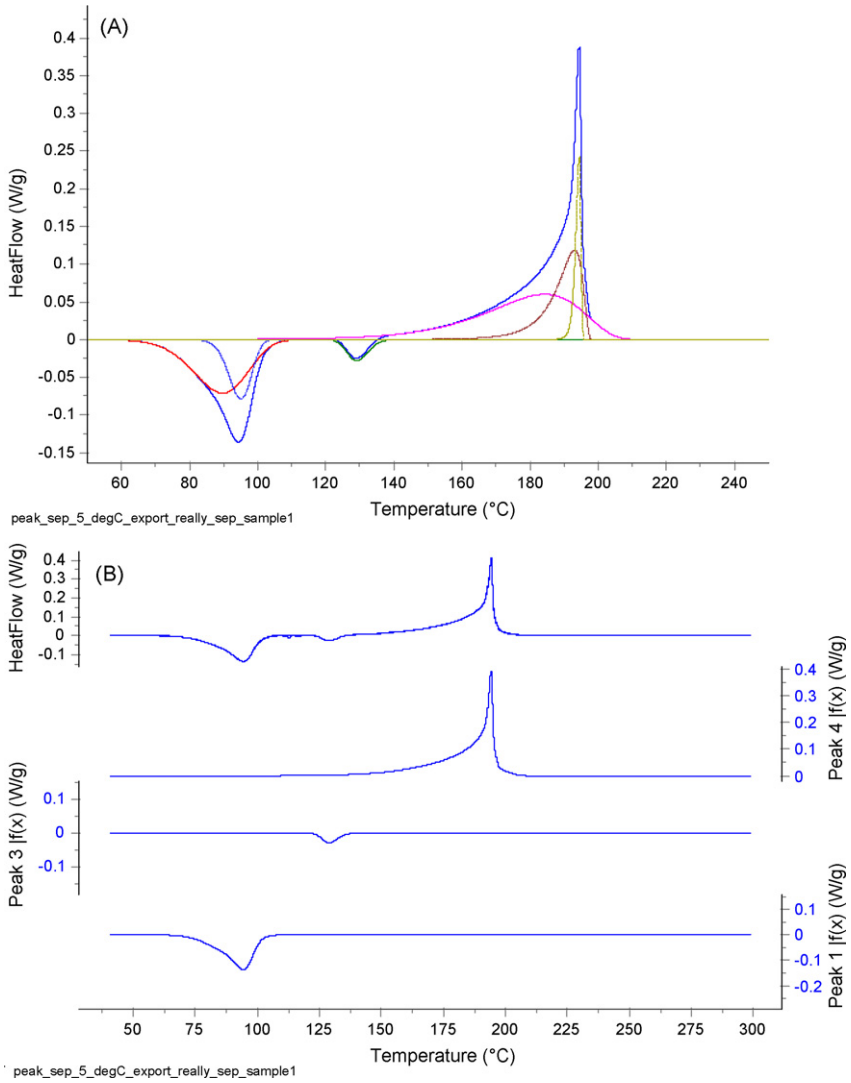

Fig. 5. Peak separation of DSC signals prior to kinetic analysis: (A) asymmetric Gaussian type signals are fitted to the obtained DSC signals; (B) the resulting peaks separation.

in Fig. 7. Comparison between actual and predicted DSC signal is depicted in Fig. 8 for the different samples. In general for each sample, kinetic analysis of the second endothermic event revealed similar behavior to first endothermic event; for brevity, plots for the second endothermic event are not shown here. Table 2 summarizes the overall enthalpy changes and apparent activation energy range for different thermal events.

3.3.1. Endothermic events

The enthalpy change values presented in Table 2 for the endothermic event shows that the heat absorption decreases in the order: sample 1 > sample 4 > sample 2 > sample 3. Apparently, this order does not correlate with the sample's mineralogy due to the interplay of other factors, such as variation in sample's particle size distribution. Experimental work is in progress to isolate sample's mineralogy and particle size distribution to study the separate effects of each parameter on sulfide mineral oxidation. This will be reported in future papers.

3.3.1.1. Prediction under different temperature regimes for endothermic events. Predictions of a given sample's stability are made under different temperature regimes using the kinetic parameters. Such predictions enable quantification of sample's degradation under temperature regime of interest. Fig. 9 depicts isothermal prediction from 50 to 90 °C for the first endothermic event. At 90 °C, the endothermic event with sample 1 is completed within 4 min, taking about twice as long with other samples. However, at lower temperatures, sample 1 took a longer time than others to achieve equivalent percent degradation. This fact is better depicted by the real-life daily temperature variation of Quebec – a transit point during shipment of the mineral concentrates (Fig. 10). At the temperature conditions of Quebec, only a 25% conversion was simulated with sample 1 after 3 years, whereas samples 2–4 reached 100% conversions within 100 days. Thus, these results imply that samples 2–4 exposed to oxygen environment in Quebec for 4 months will attain 100% reaction progress of this event, i.e., the endothermic event would no longer be observable with a repeated DSC test under similar conditions after 4 months. However, since the concentrates are stored in air environment (≈21% O_2) rather than pure oxygen, the endothermic degradation will take much longer time. Nonetheless, with the prediction in pure O_2 been more conservative than in air (e.g., as shown in Fig. 3 and Ref. [10]), the present result is on a safer side of the thermal stability screening.

3.3.2. Exothermic events

This section discusses kinetic analysis of the exothermic events for the concentrate samples, and possible effects of procedural variables on the kinetic results. As shown in Fig. 11, the apparent

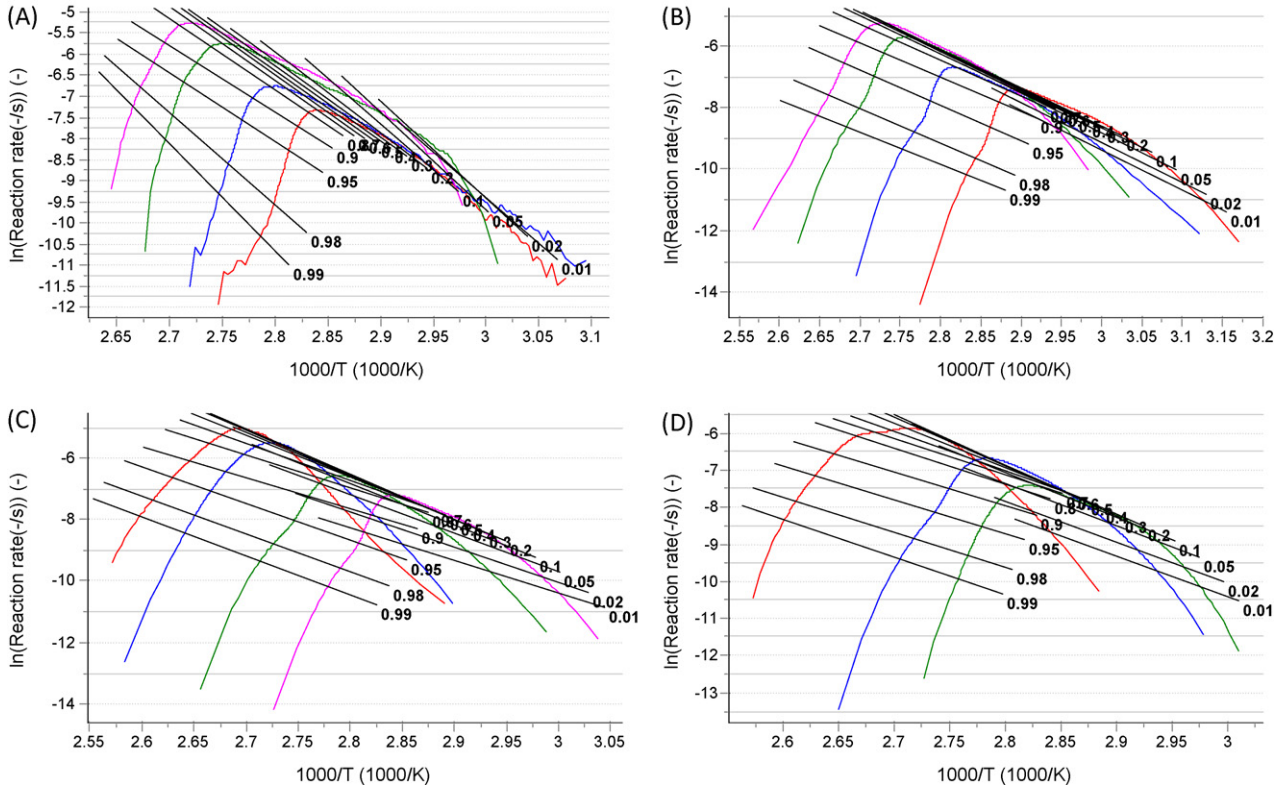

Fig. 6. Differential iso-conversional plots of first endothermic event: (A) sample 1; (B) sample 2; (C) sample 3; (D) sample 4.

activation energy plots revealed some similarities for samples 1 and 2 within reaction progress of $5\% < \alpha < 85\%$. With both samples, multiple changes of apparent activation energy are evident, with sharp decrease at $\alpha \approx 85\%$. However, while this decrease continued towards the end of reaction with sample 1, it increased prior to reaction completion with sample 2. Often a sudden decrease in apparent activation variation with reaction progress signifies auto-ignition (or auto-catalysis) with iso-conversional approach.

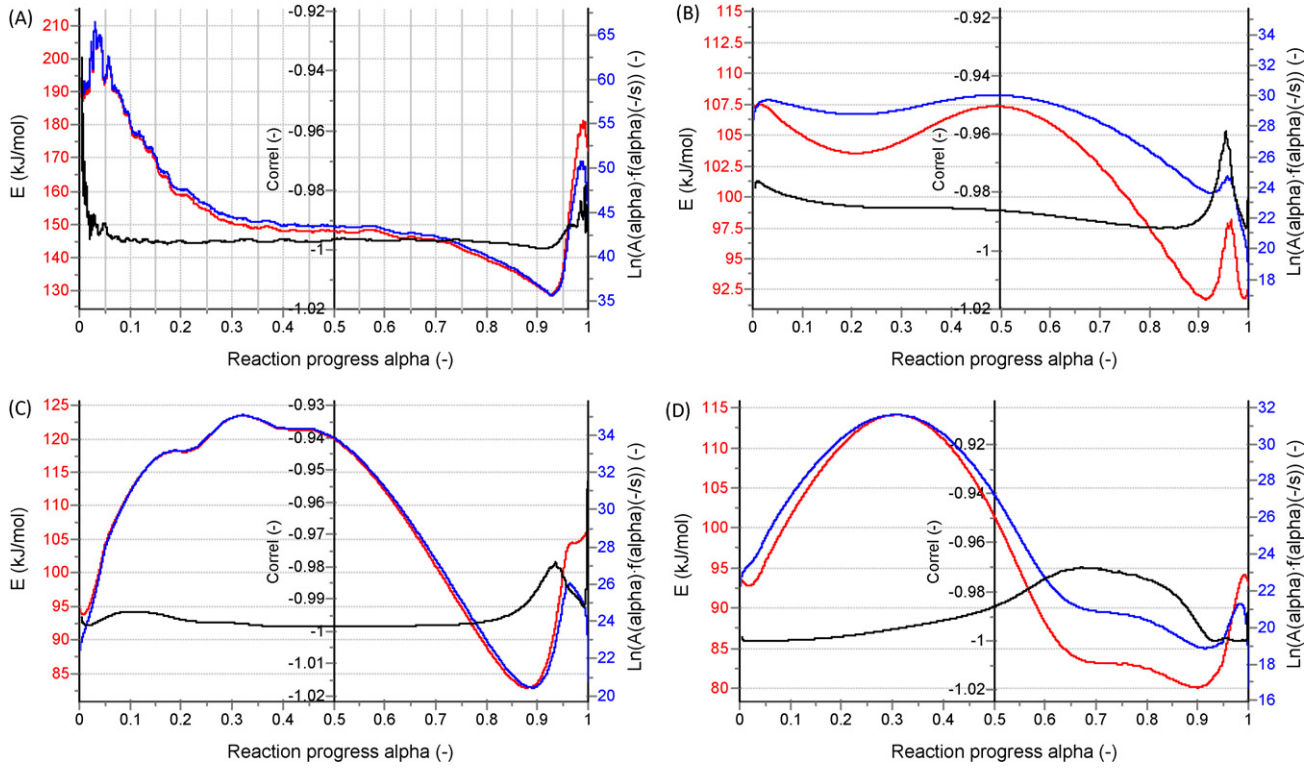

Fig. 7. Apparent activation energy, preexpoenential factor, and correlation variation as function of reaction progress of the first endothermic event: (A) sample 1; (B) sample 2; (C) sample 3; (D) sample 4.

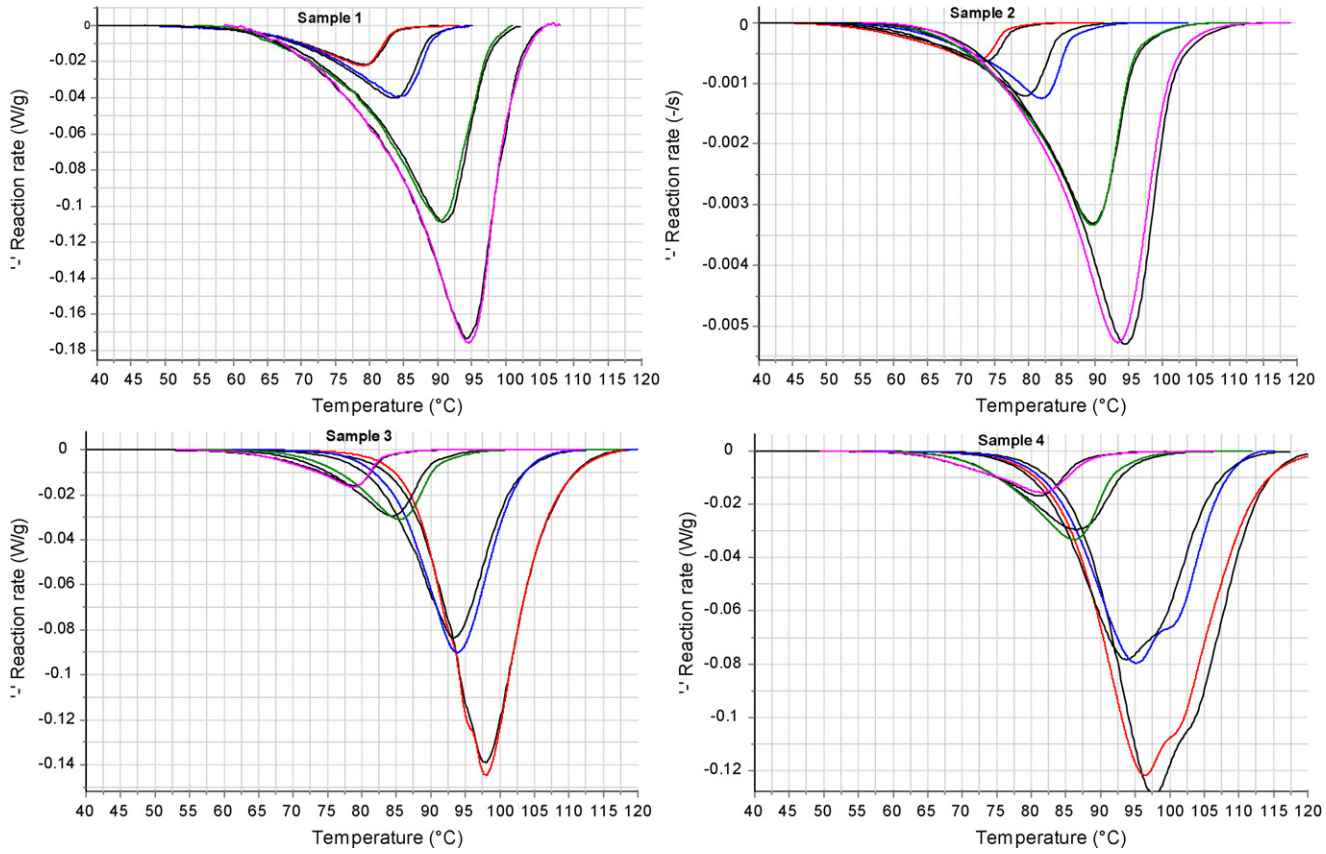

Fig. 8. Comparsion between experimental (colored lines) and predicted (black lines) normalized reaction rates of the first endothermic event.

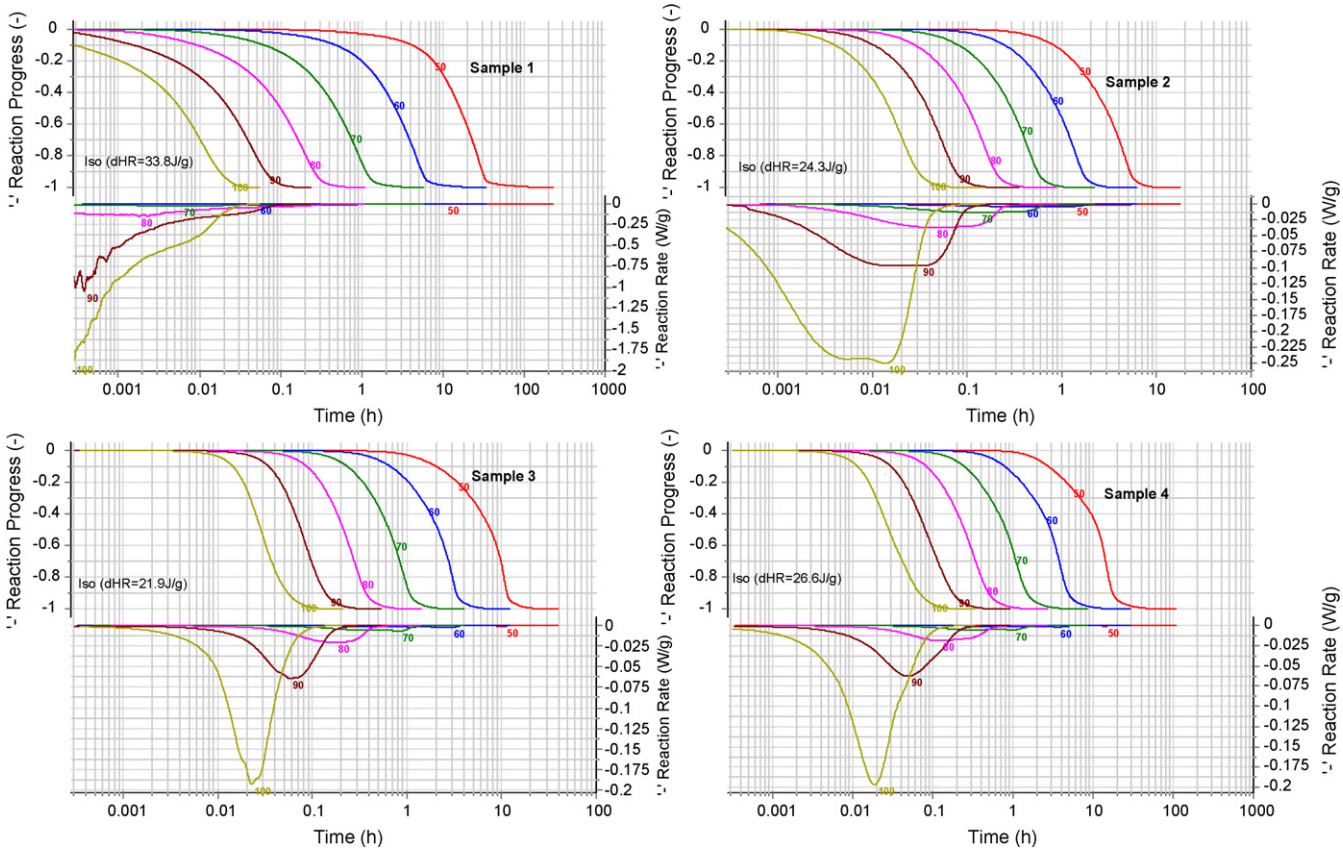

Fig. 9. Simulated reaction progress/rates of the first endotherm under different isothermal conditions.

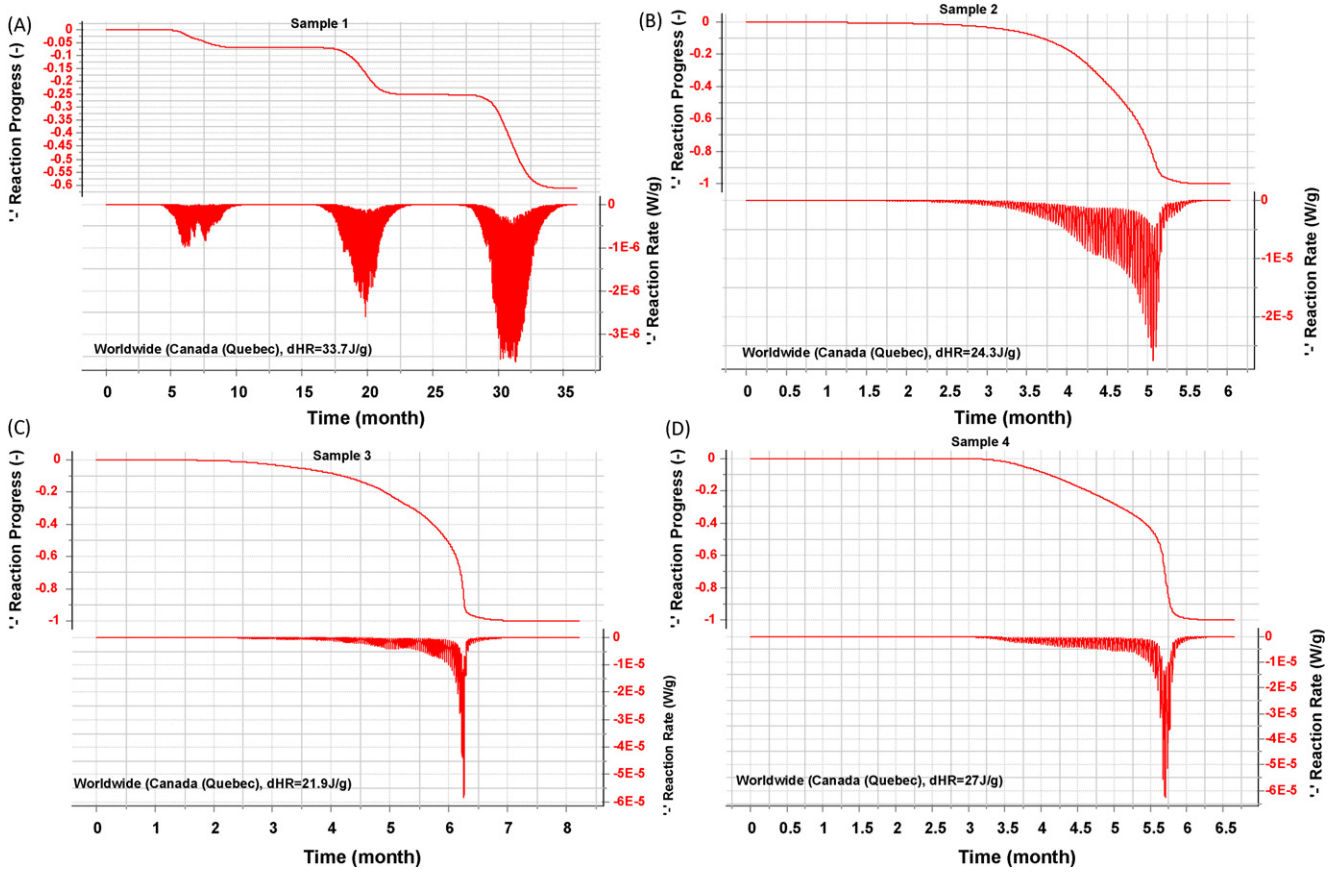

Fig. 10. Simulated reaction progress/rates of the first endothermic event under real-life Quebec temperature conditions: (A) sample 1; (B) sample 2; (C) sample 3; (D) sample 4.

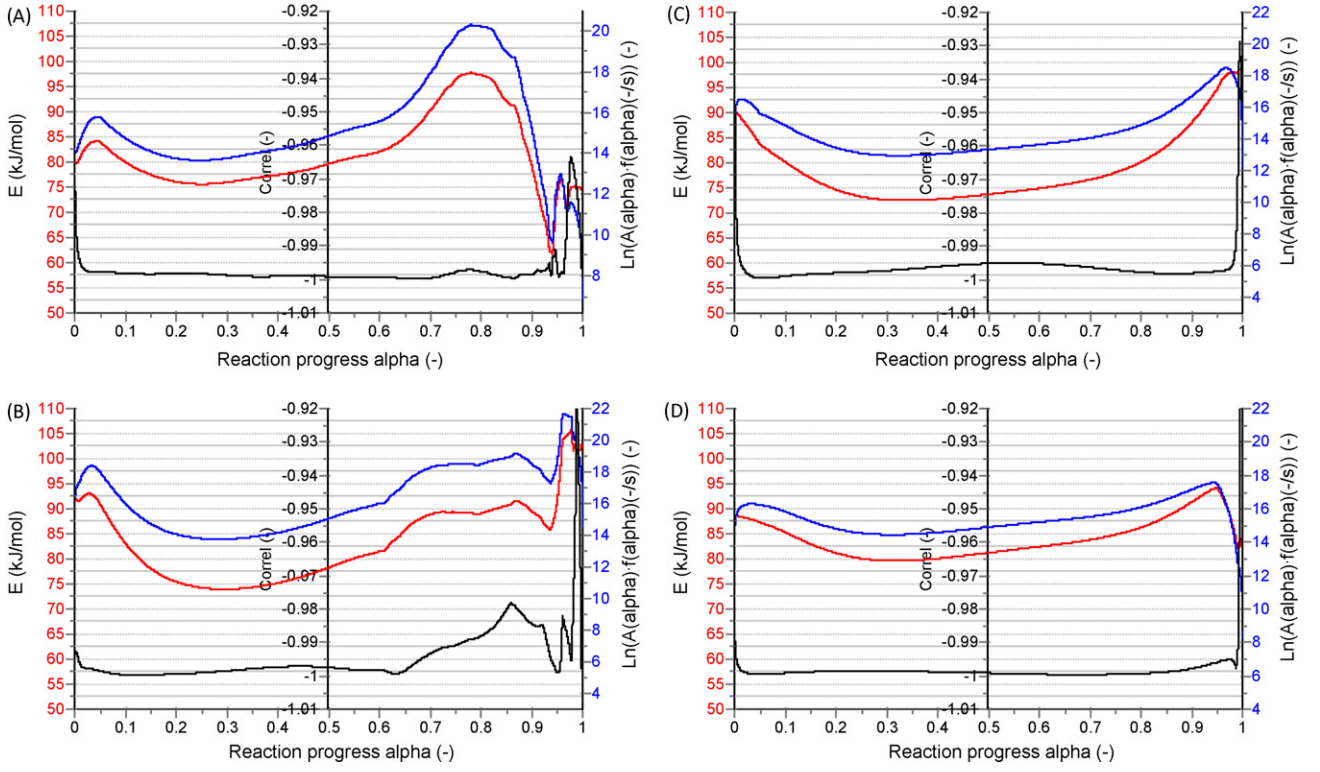

Fig. 11. Apparent activation energy variation as function of reaction progress of the exothermic event: (A) sample 1; (B) sample 2; (C) sample 3; (D) sample 4.

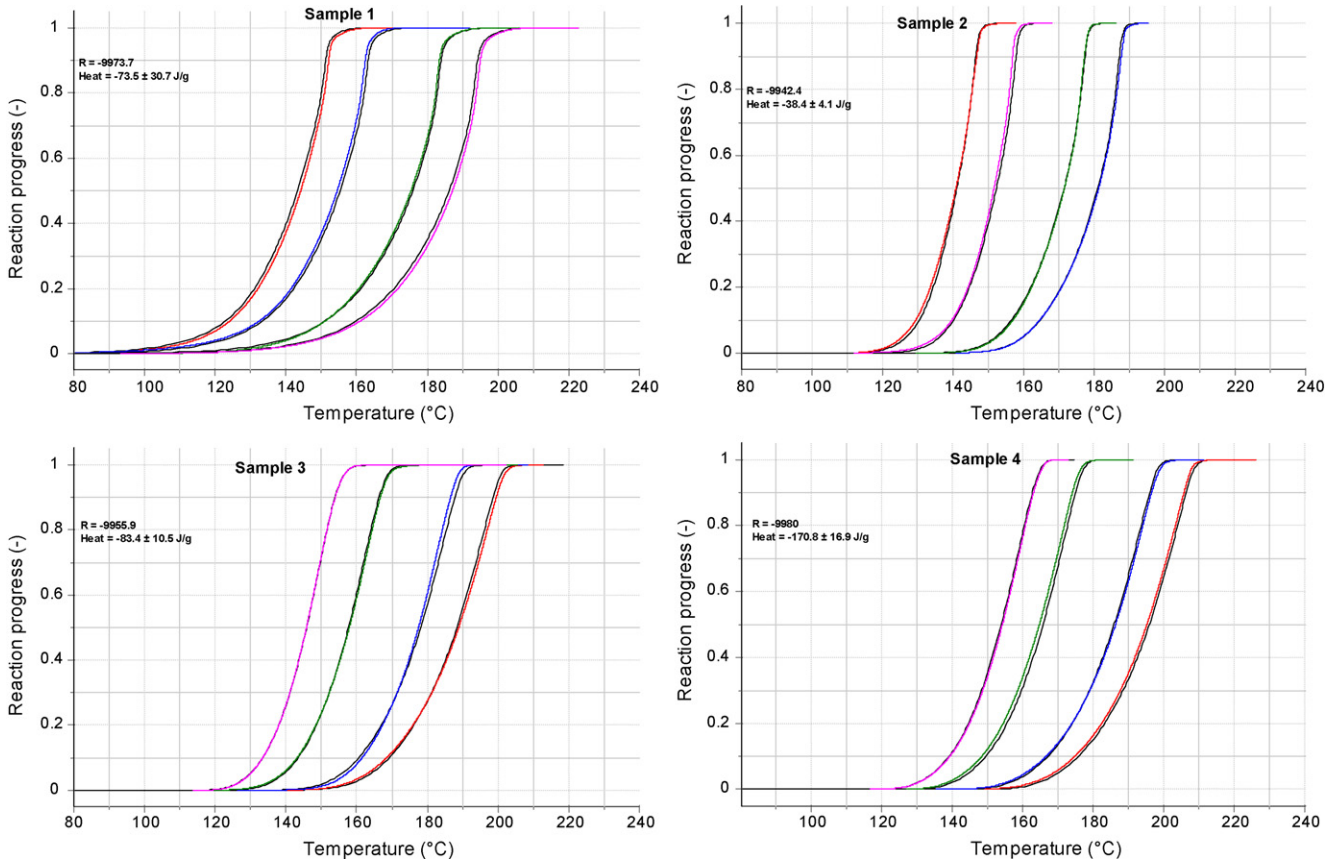

Fig. 12. Comparsion between experimental (colored lines) and predicted (black lines) reaction progress of the exothermic event.

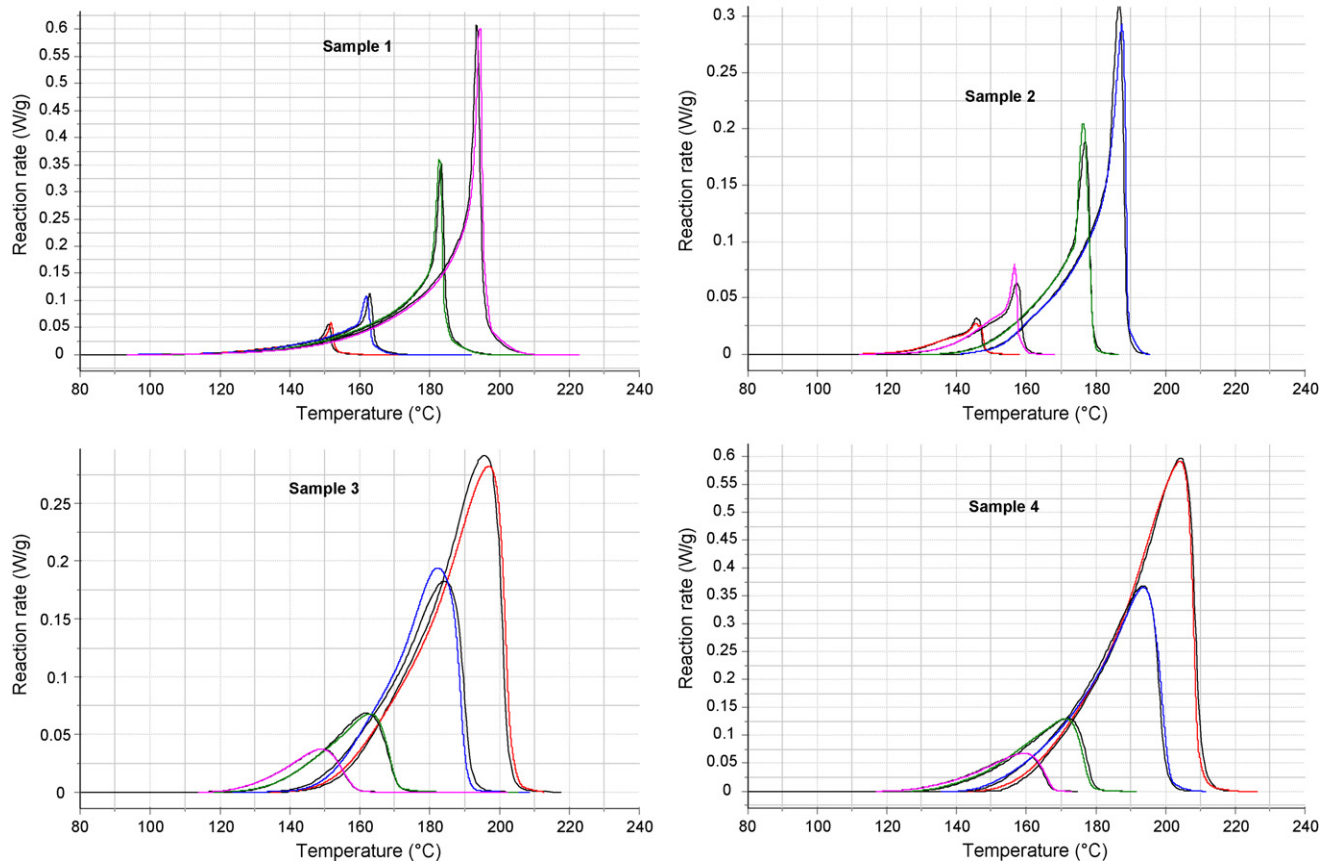

Fig. 13. Comparsion between experimental (colored) and predicted (black) normalized reaction rates of the exothermic event.

Samples 3 and 4 with larger and comparable particle size range (80–110 μm) show similar apparent activation energy trends with reaction progress. Both samples featured two major exothermic activities between 5% < α < 95%; the first characterized by decreased apparent activation energy until about 30% of the reaction progress, whereas the second event shows a gradual increase in apparent activation energy. With relatively larger particles of samples 3–4, the foregoing observations are expected because from thermodynamic standpoint, the partial pressure oxygen will influence slightly the beginning of the oxidation. Of course, later and mainly from oxygen diffusional reasons, oxygen rate will be faster and reaction rate increasing tremendously as characterized by apparent activation energy decrease.

The comparison of the experimental data with the simulated course of reaction progress and reaction rate from the obtained kinetic parameters is depicted in Figs. 12 and 13 respectively. In agreement with the apparent activation energy plots, reaction rates presented in Fig. 13 clearly show similarity in the exothermal events in the two categories of samples, i.e., samples 1–2, and samples 3–4. Additionally, the proper simulation of the obtained reaction progress/rates further demonstrates the versatility of proposed kinetic approach, which is further validated with isothermal measurements data in the next section.

3.3.3. *Validation of kinetic analysis*

In previous sections, we have demonstrated a unique approach to iso-conversional kinetic analysis, involving peak separation subsequent to endo/exothermal peak analysis. However, it is imperative to validate this approach with measured isothermal and/or adiabatic tests to further provide confidence with the method. Comparison of predicted adiabatic modes from kinetic results of this study with measured adiabatic data in Accelerating Rate Calorimeter (ARC) and Advanced Reactive System Screening Tool (ARSST) would be investigated in future work. For the present paper, validation of kinetic results with isothermal measurement at 145, 160 and 175 °C under similar gas environment is provided. Such validation are typically achieved in two ways:

(1) using kinetics obtained from non-isothermal measurements to make isothermal predictions and comparing such predictions with measured isothermal data;
(2) obtaining kinetics from measured isothermal data for comparison with the obtained kinetics from non-isothermal measurements.

The first validation is rather straightforward and commonly used, however, due to the temperature fluctuations, precise overlaps of measured isothermal data with predictions from non-isothermal kinetics are sometimes difficult to achieve. This is because the kinetic prediction assumes ideal isothermal conditions, which is often not the case with most simple calorimetric instruments. The second validation method is quite challenging due to difficulty in obtaining appropriate baseline with isothermal data. Isothermal measurements are characterized by large initial temperature jump hampering onset baseline behavior (Fig. 14) – a requirement for accurate kinetic analysis. Although this difficulty could be overcame by performing the isothermal measurements at low temperature to capture reaction onset, however this would be impractical due to long testing time and/or poor instrument sensitivity. For instance, if an isothermal measurement were to be made on with sample 1 at 40 °C, it will take over 2 months for the exothermic reaction to reach completion!

To address this problem, the kinetic analysis was performed with combined isothermal and non-isothermal data simultaneously as proposed by other authors [19–21]. Fig. 14 compares

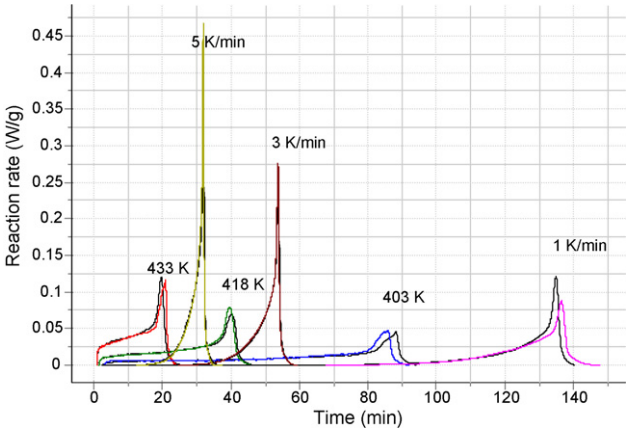

Fig. 14. Simultaneous simulation of isothermal and non-isothermal reaction rates using "combined-kinetic" approach for the exothermic event. Experimental (colored); simulations (black).

the predicted DSC signals with the isothermal and non-isothermal experimental data. The obtained isothermal and non-isothermal measurement compare fairly well with the predictions using combined-kinetic approach. Note the steepness in the baseline of isothermal signals in the initial region, which would have made it difficult to obtain good baseline optimization for the isothermal measurements. However, with the "combined-kinetic" approach the behavior of isothermal baseline are easily inferred from the non-isothermal baseline since the latter is known to a high degree of accuracy. Additionally, it can be envisaged that the obtained kinetics from the "combined-kinetic" approach will be more robust than the kinetics from either dynamic or isothermal measurements alone due to synergistic benefits of covering different temperature regimes. However, further work will be required to elucidate this point, which could constitute a subject of future research.

4. Conclusions

Sulfide minerals stability has been investigated using DSC techniques in the presence of oxygen. The MLA revealed pentlandite as the main sulfide phase with smaller grains of pyrrhotite, chalcopyrite and cubanite. BSE images show preferential oxidization of concentrate particles along certain crystallographic planes different from previously reported BSE images for sulfide mineral ores that occurs along particle margins. An improved iso-conversional approach involving peak separation, individual peak analysis and combination of isothermal/non-isothermal regimes was applied. This kinetic approach was demonstrated to be effective for investigating and predicting the thermal behavior of complex solid reactions using sulfide mineral oxidation as case study.

Acknowledgements

The authors wish to thank Dr. Bertrand Roduit for valuable discussions and help with AKTS software. We also like to acknowledge Dr. Lawrence Cochrane for his revision and valuable comments on this paper, and finally we thank Vale-Inco for supplying samples and providing financial support.

References

[1] J.G. Dunn, The oxidation of sulphide minerals, Thermochimica Acta 300 (1997) 127–139.
[2] J.G. Dunn, J.H. Sharp, Thermogravimetry, in: J.D. Winefordner (Ed.), Treatise on Analytical Chemistry, vol. 13, John Wiley & Sons, New York, 1993, pp. 127–266.
[3] P.J. Haynes, Thermal Methods of Analysis, Blackie Academic and Professional, London, UK, 1995.

[4] Z.D. Zivkovic, N. Mitevska, V. Savovic, Kinetics and mechanism of the chalcopyrite-pyrite concentrate oxidation process, Thermochimica Acta 283 (1996) 121–130.
[5] S.V. Vyazovkin, A.I. Lesnikovich, Error in determining activation-energy caused by the wrong choice of process model, Thermochimica Acta 165 (1990) 11–15.
[6] S. Vyazovkin, Evaluation of activation energy of thermally stimulated solid-state reactions under arbitrary variation of temperature, Journal of Computational Chemistry 18 (1997) 393–402.
[7] AKTS, Advanced Kinetics and Technology Solutions. http://www.akts.com (AKTS – Thermokinetics and Thermal Safety Software).
[8] P.G. Thornhill, L.M. Pidgeon, Micrographic study of sulfide roasting, Transactions of the American Institute of Mining and Metallurgical Engineers 209 (1957) 989–995.
[9] J.G. Dunn, L.C. Mackey, The measurement of ignition temperatures and extents of reaction on iron and iron–nickel sulfides, Journal of Thermal Analysis 37 (1991) 2143–2164.
[10] B. Roduit, M. Maciejewski, A. Baiker, Influence of experimental conditions on the kinetic parameters of gas–solid reactions—parametric sensitivity of thermal analysis, Thermochimica Acta 283 (1996) 101–119.
[11] H.P. Wang, A review on process-related characteristics of pyrrhotite, Mineral Processing and Extractive Metallurgy Review 29 (2008) 1–41.
[12] H.P. Wang, A. Pring, Y.N. Xie, Y. Ngothai, B. O'neill, Phase evolution and kinetics of the oxidation of monosulfide solid solution under isothermal conditions, Thermochimica Acta 427 (2005) 13–25.
[13] N. Belzile, Y.W. Chen, M.F. Cai, Y.R. Li, A review on pyrrhotite oxidation, Journal of Geochemical Exploration 84 (2004) 65–76.
[14] M.P. Janzen, R.V. Nicholson, J.M. Scharer, Pyrrhotite reaction kinetics: reaction rates for oxidation by oxygen, ferric iron, and for nonoxidative dissolution, Geochimica et Cosmochimica Acta 64 (2000) 1511–1522.
[15] R.V. Nicholson, J.M. Scharer, Laboratory studies of pyrrhotite oxidation-kinetics environmental, Geochemistry of Sulfide Oxidation 550 (1994) 14–30.
[16] T. Tanabe, K. Kawaguchi, Z. Asaki, Y. Kondo, Oxidation-kinetics of pentlandite, Journal of the Japan Institute of Metals 50 (1986) 720–726.
[17] J.G. Dunn, C.E. Kelly, A TG-MS and DTA study of the oxidation of pentlandite, Journal of Thermal Analysis 18 (1980) 147–154.
[18] B. Roduit, L. Xia, P. Folly, B. Berger, J. Mathieu, A. Sarbach, H. Andres, M. Ramin, B. Vogelsanger, D. Spitzer, H. Moulard, D. Dilhan, The simulation of the thermal behavior of energetic materials based on DSC and HFC signals, Journal of Thermal Analysis and Calorimetry 93 (2008) 143–152.
[19] A.K. Burnham, L.N. Dinh, A comparison of isoconversional and model-fitting approaches to kinetic parameter estimation and application predictions, Journal of Thermal Analysis and Calorimetry 89 (2007) 479–490.
[20] B. Roduit, Computational aspects of kinetic analysis. Part E: the ICTAC kinetics project—numerical techniques and kinetics of solid state processes, Thermochimica Acta 355 (2000) 171–180.
[21] B. Roduit, C. Borgeat, B. Berger, P. Folly, B. Alonso, J.N. Aebischer, The prediction of thermal stability of self-reactive chemicals—from milligrams to tons, Journal of Thermal Analysis and Calorimetry 80 (2005) 91–102.